Watermarking-Based Blind QoS Assessment for Wireless Image Communication

Hongxia Wang and Bangxu Yin
School of Information Science and Technology, Southwest Jiaotong University, Chengdu, 610031, China
Email: {hxwang, bxyin}@home.swjtu.edu.cn

***Abstract*—This paper presents a novel scheme to blindly estimate the quality of an image communication link by means of an unconventional use of digital watermarking. The watermarking technique is usually employed for digital media copyright protection and authenticity verification. However, watermarking is here adopted as a method to provide a blind assessment of the quality of service (QoS) in wireless image communication. First, a compressed-domain watermarking scheme is proposed. Each 8×8 block in a JPEG compressed image is first processed by entropy decoding, and then the parity of the number of non-zero alternating current (AC) coefficients in each quantized discrete cosine transform (DCT) block is modified to embed the watermark. Second, the performances of the proposed watermarking scheme have been tested. Finally, the proposed watermarking scheme is applied to estimate the QoS of an image communication link based on the assessment factor which is associated with the errors between the extracted watermark and the original. Experimental results show the proposed scheme can evaluate the QoS of wireless image communication channels exactly without increasing the bit rate transmission. Moreover, the quality of the carrier image has not been affected.**

***Index Terms*—Image communication, quality of service, digital watermarking, compressed-domain**

I. Introduction

Recently, more and more mobile telephones are used in our daily life. Moreover, the functions of a mobile telephone are more and more advanced with growth of software and hardware techniques. Specially, quite a number of mobile telephones can take a photo, which makes the users share their photos by sending and receiving digital images each other. Therefore, the image transmission over wireless communication channel is very popular. With phenomenal growth in wireless image communication, the issues need to handle are resource consumption and the quality of the image being transmitted in wireless channels. To meet the requirements of the popular image communication via mobile telephones or non-ideal channels with a higher bit error rate (BER), a watermarking-based blind quality of service (QoS) assessment method for wireless image communication is proposed in this paper.

As a common image format in the application, JPEG compression standard is especially designed for transmitting images over wire channel. During JPEG compression, the image is first divided into disjoint 8×8 pixel blocks. Each block is transformed using the discrete cosine transform (DCT). The DCT coefficients are then divided by quantization steps stored in the quantization matrix and rounded to integers. The JPEG compression finishes by ordering the quantized coefficients along a zig-zag path, encoding them, and finally applying lossless compression. On the contrary, the JPEG decompression works in the opposite order.

It is well known that the Huffman coding in JPEG compression process is very sensitive to the bitstream error, thus it is difficult to transfer JPEG image with a high error rate. Consequently, JPEG coding standard is not adaptive to transmit an image over wireless channel with a higher error rate. However, 3G mobile communication systems are expected to offer multimedia applications and services with negotiation end-to-end QoS. As a kind of important multimedia application, the JPEG image service such as transmission, share and storage is accepted by more and more users. Therefore, it is necessary that service providers develop simple and effective billing systems related to the quality of the services supplied. It is then crucial to devise quality assessment systems that do not increase the bit rate transmission [1].

In these years, digital watermarking is a useful solution for multimedia copyright protection and authenticity verification [2]-[5], and it has been a popular research topic. However, most watermarking related literature focuses on how to resist deliberate attacks by applying benchmarks to watermarked media that assess the effectiveness of the watermarking algorithm, while only a few papers have concentrated on the blind measure of the quality of service in multimedia communications. Furthermore, most carrier signals of existing schemes are video sequences for purpose of assessing the quality of service [6]-[9], while that of the image as a carrier signal is less. In [6], an unconventional use of a fragile watermark to evaluate the QoS in multimedia mobile communications was presented. Like a tracing signal, the

Manuscript received February 2, 2013; revised March 25, 2013.
This research was supported by the National Natural Science Foundation of China (NSFC) under Grant No. 61170226, the Fundamental Research Funds for the Central Universities under Grant Nos. SWJTU11CX047, SWJTU12ZT02, the Young Innovative Research Team of Sichuan Province under Grant No.2011JTD0007, and Chengdu Science and Technology Program under Grant No. 12DXYB214JH-002.
Corresponding author email: hxwang@home.swjtu.edu.cn.
doi:10.12720/jcm.8.3.207-215.

watermark tracked the data, where it was embedded, since both the watermark and the host data followed the same communication link. The estimation of the tracing watermark allowed dynamically evaluating the effective quality of the provided video services. The sensitivity of the detected tracing watermark on the quality of service indices provided for some useful capabilities for analyzing future mobile universal mobile telecommunications system (UMTS) services. However, the effect of computational complexity caused by watermark embedding had not been considered during the video transmission in real time. Ref. [7] focused on QoS assessment of 3G video-phone calls by tracing watermarking. In [7], a color space was adopted to minimize the perceptual distortions introduced by digital watermarking. Analytical results show the benefits obtained in tracing watermarking by the new representation color space. In addition, In [8] and [9], authors proposed a business model for video-call billing for end-to-end QoS provision by employing the watermark to monitor the QoS of the communication link. Therefore, the network operator is able to implement an adaptive billing strategy by depending on the effective received quality and maximizing the profit.

Above mentioned tracing watermarking-based QoS assessment schemes are all video sequences as the carrier signals. However, these methods are not directly suitable for JPEG image. In [10], the authors proposed an image watermarking scheme that can work as an automatic quality monitoring system. The watermark is embedded into DCT domain of original image, and the DCT blocks for embedding are carefully selected so that the degradation of the watermark can reflect the degradation of the image. In addition, the compressed-domain fragile watermarking schemes were presented in [11] and [12]. These fragile watermarking schemes addressed to detect and locate various malicious tampering of protected images. For less channel quality evaluation schemes aiming at JPEG image, it is highly desirable to develop QoS assessment for JPEG image transmission over wireless channel by tracing watermarking.

In this paper, we propose a blind QoS assessment scheme for JPEG image communication using tracing watermarking. In our scheme, an image encoded by means of the JPEG compression standard are considered as host data. Based on the quantized DCT coefficients blocks after JPEG decoding, a compressed-domain watermarking algorithm is proposed. The watermark is embedded into each DCT block by modifying the parity of the number of non-zero AC (alternating current) coefficients. Furthermore, the changes of the image quality and the length of coding bitstream due to watermark embedding are all analyzed. The watermarked data are coded and transmitted over a simulated noisy channel. At the receiving side, according to the errors between the extracted watermark and the original, we can effectively evaluate the quality of the communication channel using the defined assessment factor. Moreover, our scheme does not affect the quality of the carrier images, as well as need not extra payloads for the introduced watermark data.

II. Proposed Compressed-Domain Watermarking Algorithm

This section describes in detail the proposed compressed-domain watermarking algorithm, which includes watermark embedding and extracting process, and the performance analysis. If the watermark is processed directly in the JPEG lossy compressed image, due to the quantization and requantization of DCT coefficients carrying some unavoidable quantization error, there will be great influence on tracing watermark. A good idea is that the watermark is added directly to the quantized DCT coefficients in order to resolve this problem, i.e. using the compressed-domain watermarking technique. Firstly, we decode the JPEG image, and then obtain many 8×8 quantized DCT blocks. After that, we modify the parity of the number of non-zero quantized AC coefficients in each 8×8 DCT block for watermark embedding. In order to inspect whether the proposed watermarking scheme meets to evaluate the quality of JPEG image communication link or not, the performances such as imperceptibility and the changes of the length of coding bitstream due to watermark embedding are all tested.

A. *Watermark Embedding and Extracting in Compressed-Domain*

JPEG image compression process consists of conversion of RGB to YUV mode, composition of the minimum coding unit (MCU), 2-D DCT, quantification of DCT coefficients, run-length coding and Huffman coding [13]. In this paper, the watermark will be embedded into the quantized DCT coefficients blocks. Because the direct current (DC) components are perceptually significant than AC components, if we modify the quantized DC components, the visual quality of watermarked image will be degraded largely. So we embed the watermark information into AC components to meet the requirement of invisibility. Watermarking embedding is according to the number of non-zero quantized AC coefficients in every 8×8 DCT block. As we know, there are 63 quantized AC coefficients denoted by $C_1, C_2, \cdots, C_{63}$ in each corresponding 8×8 DCT block. We calculate

$$N_{AC} = \mathrm{nnz}(C_1, C_2, \cdots, C_{63}) \qquad (1)$$

where $\mathrm{nnz}(\cdot)$ represents the number of non-zero elements. Then, the binary watermark $W = \{w_1, w_2, \cdots, w_n\}$, $w_i \in \{0,1\}$ is embedded into each DCT block according to the following rule:

$$\begin{cases} w_i = 0 \Leftrightarrow N_{AC}\ is \quad \text{even} \\ w_i = 1 \Leftrightarrow N_{AC}\ is \quad \text{odd} \end{cases}, \qquad i = 1, 2, \cdots, n \qquad (2)$$

To embed the watermark information, we search for the last non-zero quantized AC coefficient C_l in a zig-zag scan order shown in Fig. 1 and modify it as follows:

$$\begin{cases} C'_l = 0, & \text{if } (C_l = \pm 1 \,\&\, \mathrm{mod}(N_{Ac},2) = 1 \,\&\, w_i = 0) \\ C'_l = C_l \text{ and } C'_{l+1} = 1, & \text{if } (C_l \neq \pm 1 \,\&\, \mathrm{mod}(N_{Ac},2) = 1 \,\&\, w_i = 0) \\ C'_l = 0, & \text{if } (C_l = \pm 1 \,\&\, \mathrm{mod}(N_{Ac},2) = 0 \,\&\, w_i = 1) \\ C'_l = C_l \text{ and } C'_{l+1} = 1, & \text{if } (C_l \neq \pm 1 \,\&\, \mathrm{mod}(N_{Ac},2) = 0 \,\&\, w_i = 1) \\ C'_l = C_l, & \text{otherwise} \end{cases} \tag{3}$$

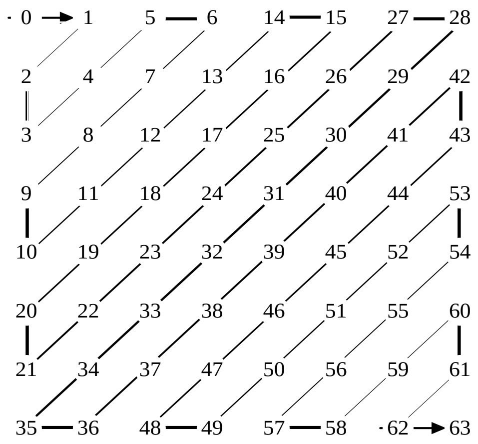

Figure 1. Zig-zag scan order.

The procedure of watermark embedding is performed by modifying the last non-zero quantized AC coefficient C_l as formula (3). On one hand, for each 8×8 quantized DCT block, if we embed the watermark bit 0, and the number of non-zero quantized AC coefficients N_{AC} is odd, i.e. mod(N_{AC},2)=1, N_{AC} should be modified to the even value according to formula (2). According to this rule, we modify C_l to be zero when $C_l = \pm 1$. Thus N_{AC} will be changed to the even value; when $C_l \neq \pm 1$, we modify the next element of C_l to 1, i.e., let $C_{l+1} = 1$. Thus N_{AC} will also be changed to the even value. On the other hand, if we embed the watermark bit 1, and N_{AC} is even, N_{AC} should be modified to the odd value according to formula (2). According to this rule, we modify C_l to be zero when $C_l = \pm 1$. Thus N_{AC} will be changed to the odd value; when $C_l \neq \pm 1$, we modify the next element of C_l to 1, i.e., let $C_{l+1} = 1$. Thus N_{AC} will also be changed to the odd value. For other case, the parity of N_{AC} is accordance with that of the watrmark bit, so C_l will not been changed .

For example, as shown in Fig. 2(a), the original 8×8 DCT block has 6 non-zero quantized AC coefficients, i.e., $N_{AC} = 6$. The last non-zero quantized AC coefficient C_l lies in the coordinate (1,5) according to zig-zag path shown in Fig. 1. Because of $\mathrm{mod}(N_{AC},2) = 0$ and $C_l = -1$, if we embed the watermark bit 0, the last non-zero quantized AC coefficient C_l will not be modified according to the formula (3). But if we embed the watermark bit 1, we need modify the value of C_l to be 0 following the formula (3). The watermarked DCT block is shown in Fig. 2(b).

C_l

DC	2	-1	0	**-1**	0	0	0
1	0	-1	-1	0	0	0	0
0	0	0	0	0	0	0	0
0	0	0	0	0	0	0	0
0	0	0	0	0	0	0	0
0	0	0	0	0	0	0	0
0	0	0	0	0	0	0	0
0	0	0	0	0	0	0	0

(a) Original quantized DCT block

C'_l

DC	2	-1	0	**0**	0	0	0
1	0	-1	-1	0	0	0	0
0	0	0	0	0	0	0	0
0	0	0	0	0	0	0	0
0	0	0	0	0	0	0	0
0	0	0	0	0	0	0	0
0	0	0	0	0	0	0	0
0	0	0	0	0	0	0	0

(b) Watermarked DCT block

Figure 2. An example for describing the modification of the last non-zero quantized AC coefficient due to watermark bit 1 embedded into an 8×8 DCT block.

At the sending side, the sender transmits the watermarked image bitstream over wireless channel. Because the 8×8 block is the minimum coding unit of an image, we use the 8×8 block shown in Fig. 2 as an example. After watermark embedding, the watermarked 8×8 DCT block shown in Fig. 2(b) is scanned in a zig-zag order employing run-length encoding (RLE) algorithm that groups similar frequencies together, and the sequence becomes (DC,2,1,0,0,–1,0,–1,0,0,0,0,0,–1, 0,…,0). Then, the DC coefficient is encoded by prediction difference method. That is to say, the previous quantized DC coefficient is used to predict the current quantized DC coefficient. The difference between the two is encoded rather than the actual value. For example, the difference of DC coefficients between two adjacent 8×8 quantized DCT blocks is –27. From the Huffman Table [14] [15], this difference value corresponding Huffman code word is "11000011". The remaind 63 AC coefficients are encoded to be (0,2); (0,1); (2,–1); (1,–1); (5,–1); *EOB* by RLE. Here, EOB represents the end of block, and its latter coefficients are all zeros. Then, we perform the entropy coding according to the Huffman Table [14] [15], and obtain the corresponding Huffman code words as follows: (0,2)→01+10; (0, 1)→ 00+01; (2,–1)→11011+10; (1,–1)→1100+10; (5,–1)→ 1111010+10; EOB→1010. Here, the supplement bits "+10" and "+01" are added for more precision purpose. Thus, the whole bitstream of this 8×8 block can be obtained by combining in succession these Huffman code words together. Finally, all of 8×8 blocks' Huffman code words are jointed consecutively together to form the resulting watermarked image bitstream transmitting over wireless channel.

At the receiving side, we receive the watermarked JPEG image bitstream and decode it. After decoding the Huffman code and run-length code, the 8×8 quantized DCT blocks with watermark information are obtained. Then, the watermark bit w_i' will be extracted directly from the quantized AC coefficients as follows:

$$w_i' = \begin{cases} 0, & \mathrm{mod}(N_{AC}, 2) = 0 \\ 1, & \mathrm{mod}(N_{AC}, 2) = 1 \end{cases} \quad (4)$$

For above mentioned example, the receiver can obtain the watermarked AC coefficients sequence (DC,2,1,0, 0, –1,0,–1,0,0,0,0,0,–1,0,…,0) by decoding the Huffman code and run-length code. Note that the number of non-zero quantized AC coefficients $N_{AC} = 5$, namely, N_{AC} is odd, so the extracted the watermark bit is 1 in this 8×8 DCT block. After having extracted the received watermark information for all of 8×8 DCT blocks, it is estimated and compared with the original, which is known at the receiving side, and the BER between the original watermark and the received one, is used as an index of the degradation affecting the received watermark. Our approach takes into account the evaluation of the quality of the image communication link since the watermark and the JPEG image follow the same communication link.

B. Performance Test of Proposed Watermarking Scheme

For the image quality assessment purposes, it is crucial to devise quality assessment systems that do not increase the bit rate transmission. From above described watermark embedding process, the watermark embedding is performed on the data before run-length coding and Huffman coding. Therefore, the change of coding bitstream is related with the modifications of AC coefficients due to watermark embedding.

To analyze the change of coding bitstream due to watermark embedding, the run compounding of AC coefficients in a zig-zag scan order is firstly counted. The run compounding is the process of counting the number of zero AC coefficients preceding a non-zero AC coefficient within a zig-zag scanned 8×8 DCT blocks to produce symbols representing the information of the AC coefficients themselves and the number of preceding zeros. As an example, if the quantized AC coefficients are (2,0,0,0, –3,0,0,0,0,0,0,0,0,0,0,0,0,0,0,0,1,0,…,0) in a zig-zag scan order, the run compounding will be (0,2); (3,–3); (15,1); *EOB*, and then the Huffman coding is performed on each run compounding. Finally, the coding bitstream is obtained by jointing the encoded run compounding together. According to the proposed watermarking scheme, the run compounding of the last non-zero AC coefficients in a zig-zag scan order is added 1 or removed. On the one hand, if the value 1 is added, the run compounding will be (0,1) which coding length is 3 bits, i.e., the length of coding bitstream will increase 3 bits; On the other hand, the length of Huffman coding bitstream will decrease at least 3 bits if the run compounding of the last non-zero AC coefficients is removed, because the shortest Huffman coding length is corresponding to run compounding (0,1). Obviously, other run compounding is corresponding to at least 4 bits Huffman coding, such as (1,1) corresponding to 5 bits, (1,2) corresponding to 7 bits, and (2,1) corresponding to 6 bits, and so on. From above analysis, it can be conclude that the Huffman coding length due to watermark embedding is usually shorter than that of the original. Therefore, the watermark embedding can not make the extra communication payload increase on the whole. For different images "Lenna", "Boat", "Pepper" and "Baboon" sized 512×512 and 256×256, the change of coding bitstream due to watermark embedding tabulated in Table I. Here, $L_1(b)$ represents the length of coding bitstream before watermark embedding, and $L_2(b)$ represents that of coding bitstream after watermark embedding. It can be seen that the length of coding bitstream after watermark embedding become shorter than before watermark embedding.

TABLE I. THE CHANGE OF CODING BITSTREAM DUE TO WATERMARK EMBEDDING

Image	512×512				256×256			
	Lenna	Boat	Pepper	Baboon	Lenna	Boat	Pepper	Baboon
L_1(b)	189156	216468	192648	254174	60135	66161	62181	72569
L_2(b)	180923	210197	183168	246162	57858	64230	59669	70216

As we all know, the watermark embedding affects the quality of JPEG image. In order to measure the visual indistinguishable ability, the resulting peak-signal-to-noise ratio (PSNR) due to watermark embedding is calculated. Table II lists the PSNR values of the four watermarked images sized 512×512 in this experiment. The data PSNR presents the quality of the watermarked image with respect to the original image. High values of PSNR guarantee the visual quality of the images. As shown in Table II, All PSNR values are greater than 35 dB, indicating that the watermarked images retain satisfactory visual quality, and the image distortion due to watermark embedding is small. Consequently, the watermark energy contribution for each DCT block is negligible, which makes the watermark imperceptible.

In addition, Table II also gives a performance comparison between different compressed-domain watermarking schemes, and it follows that the PSNR values of our method are similar to that of methods [11]-[12]. In [11], a compressed-domain fragile watermarking scheme for JPEG image was proposed. However, the watermark is generated by folding the hash results of quantized coefficient, and each block is used to carry two watermark bits using a reversible data-hiding method. So the sensitivity to noise is not satisfactory during image transmission. Similarly, the compressed-domain fragile watermarking algorithm for JPEG images based on chaotic system in [12] also lacks the sensitivity to noise during transmission. By using the proposed scheme, the sensitivity to noise is satisfactory due to watermark embedding into the AC components of quantized DCT coefficients blocks by formula (3). Compared to the schemes [11] and [12], the proposed watermarking scheme has a satisfactory sensitivity to noise during transmission, which is also shown in the following experimental results in Section IV.

In [11], note the index of the last non-zero coefficient in a quantized DCT block as i_{FNC} . If $i_{FNC} \le 62$, the value of $c_{i_{FNC}+1}$ or $c_{i_{FNC}+2}$ is modified according to the original LSB of two coefficients in different blocks, and the absolute value of watermarked coefficients $c'_{i_{FNC}+1}$ and $c'_{i_{FNC}+2}$ must be 1. If i_{FNC} is 63 or 64, the absolute value of i'_{FNC} must be greater than 1. Thus, the length of watermarked coding bitstream will be greater than the original in scheme [11]. Similarly, the length of watermarked coding bitstream will be increased by the scheme [12].

To sum up, from above analysis and Table II, compared to compressed-domain watermarking schemes [11]-[12], the proposed watermarking scheme cannot increase the additional data traffic when it is used to assess QoS for JPEG image transmission over wireless channel. Furthermore, the proposed scheme is capable of detecting the random noise during JPEG image transmission over wireless communication channel. At the same time, the visual quality watermarking image is satisfactory. These performances are beneficial to watermarking technique application in QoS evaluation for JPEG image transmission.

TABLE II. PERFORMANCE COMPARISONS BETWEEN OUR SCHEME AND OTHER COMPRESSED-DOMAIN WATERMARKING SCHEMES

Watermarking Scheme	PSNR due to watermarking (dB)				Sensitivity to noise during transmission	Length of watermarked coding bitstream
	Lenna	Boat	Pepper	Baboon		
Scheme in [11]	37.91	37.92	37.89	37.84	No	increasing
Scheme in [12]	34.46	33.84	32.92	33.50	No	increasing
Our scheme	42.06	36.84	35.10	38.61	Yes	decreasing

III. QUALITY OF SERVICE ASSESSMENT USING TRACING WATERMARKING

A. *Coding Transmission*

The estimation of the tracing watermark allows dynamically evaluating the effective quality of the provided image services. This depends on the whole physical layer, including the employed JPEG image coder and decoder. It is no doubt that Huffman coding is very sensitive to the bitstream error, i.e. once one incorrect bit occurs, the introduced error will spread to the decoding results of the current MCU, and even to the latter MCU. For example, if the second bit of value 20 corresponding to its Huffman code 1<u>1</u>01010100 makes a mistake, i.e. the bitstream is changed to 1<u>0</u>01010100, the decoding results will be changed to 5(100101) and –3(0100) at the decoding side. Thus, the parity of non-zero AC coefficients will be changed in the current DCT block, and the watermark cannot be extracted correctly.

To make a JPEG decoder to resynchronize after a transmission error, the JPEG standard itself allows the use of a special restart marker (RST*m*). Restart markers provide means for recovery after bitstream error, such as transmitting an image over an unreliable network or file corruption. If an image file gets corrupted, without restart markers, it will usually be corrupted from the point of the error to the end of the image; with restart markers, it will only be corrupted up to the next restart marker.

(a) Decoding “Lenna” and “Pepper” without using eight restart markers

(b) Decoding “Lenna” and “Pepper” with using eight restart markers

Figure 3. Contrast of decoding images under the condition of 1 bit error.

In general, the BER of a non-ideal channel such as wireless channel is higher than a wire channel. So we utilize restart markers to help decoder resynchronization after bitstream error. Namely, in the encoder, the eight unique restart markers in sequence from 0 to 7 (RST*m*, $m = 0,1,\ldots,7$) are periodically inserted into the entropy-coded data segments. A restart interval specifies the interval between RST*m* markers, and it is defined with the FFDD marker as a 2-byte number. This tells how many MCUs between restart markers. When the decoder encounters a restart marker (FFD0-FFD7) which exists in hexadecimal type, the DC values are reset to 0 and the bitstream is started on a byte boundary (after the FFDx). In the decoder, each scan of the compressed bitstreams is preprocessed to search all restart markers before being decoded.The insertion of restart markers into the JPEG data stream will facilitate low cost re-encoding process by stopping the propagation of errors. A typical error in the stream will have effect no further than the point where the next restart marker is detected. Consequently, the viewed image will be improved. Fig. 3 shows the decoding images “Lenna” and “Pepper” under the condition of 1 bit error. Without using eight restart markers, the decoding images are shown in Fig. 3(a), and the PSNR values are 22.13 dB and 20.42 dB, respectively. On the contrary, with using eight restart markers, the decoding images are shown in Fig. 3 (b), and the PSNR values are 35.36 dB and 29.85 dB for “Lenna” and “Pepper” image, respectively. It can be seen that the PSNRs with using eight restart markers are largely higher than without using that, which implies that the quality of the decoding images will be improved by using restart markers.

For JPEG image encoder, after each 8×8 block being entropy encoded, the bitstream data is transmitted over a noisy channel. As we know, the channel’s errors are classified into random transmission errors and burst errors. For random transmission errors, the bit errors occur randomly, i.e., the isolated bit errors occur on the random position in the data, and the bit error distributes randomly in the coding bitstream. This type of errors is usually caused by the channel’s adding Gaussian noise, and the corresponding channel is called as random error channel. For burst errors, a sequence of errors occurs during a burst error period in the data. As a rule, the first and the last bit of the data when transmitted are often in error, and some in-between bits are either correct or error, but most of bits are in error. With the burst error in the data, the output is totally changed and the receiving end has errors. This type of errors is usually caused by the channel fading in the wireless communication, and the corresponding channel is called as burst error channel. If both random transmission errors and burst errors occur in the bitstream, we call this type of error as the mixed error. In this paper, the watermarked image is transmitted over a noisy channel, and image communication is performed on mobile telephones or non-ideal channels with a higher bit error rate, such that some bits of the bitstream data are in error. So the noisy channel is simulated by generating random bit errors.

B. Decoding and QoS Evaluation

The principle idea of the tracing watermarking procedure for non-ideal wireless channel quality assessment is shown in Fig. 4. The watermark embedding is performed by our proposed algorithm for JPEG images in Section II. Obviously, the watermark is a narrow-band low energy signal. Like a tracing signal, the watermark tracks the transmitting image, where it is embedded, since both the watermark and the host image follow the same communication link.

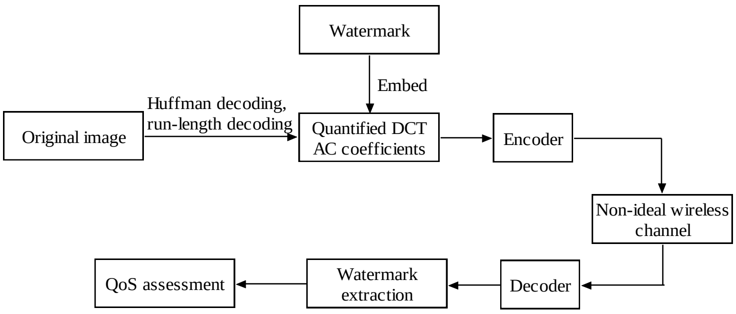

Figure 4. Principle idea of tracing watermarking for non-ideal wireless channel quality assessment in image communications.

At the receiving side, the received bitstream is firstly Huffman decoded, and then we use the restart markers to decode synchronously and control errors. In general, there are three types of errors caused by channel transmission as follows: 1) The restart markers make a mistake; 2) The block-end markers is wrong or lost; 3) The data bitstream is incorrect.

In addition, once the following cases occur, it is shown that the error has been detected. 1) If four block-end markers is decoded after a marker bit, the following bit is not the next marker; 2) When we decode AC coefficients of a DCT block, 63 AC coefficients have been obtained continuously, but any block-end marker cannot be detected; 3) The decoded AC coefficients are greater than the value 999; 4) The difference between the decoded two neighborhood restart markers is not 1. Once we detect the errors during decoding process, we will begin to search for the next marker. Simultaneously, we use a weight α to denote the degree that one wrong MCU affects the image quality, and *P* denotes the probability of wrong MCU blocks versus the overall 8×8 blocks.

After finishing the decoding process, we extract the watermark $W' = \{w'_1, w'_2, \cdots, w'_n\}$, $w'_i \in \{0,1\}$ from each 8×8 DCT block according to formula (4), then calculate DR as follows:

$$DR = \frac{\sum_{i=1}^{n}(w'_i \oplus w_i)}{n} \times 100\% \tag{5}$$

We use a weight β to denote the case of $w_i' \oplus w_i = 1$, then evaluate the quality of a image communication link by defining a assessment factor *AF*

$$AF = \alpha \cdot P + \beta \cdot DR \tag{6}$$

where, the weights α and β can be set according to the detected wrong blocks and changed watermark information. *AF* is employed to provide a quality assessment factor of the received image in the coding/transmission process. The larger *AF* indicates the lower image transfer quality. In the practical application, it can also be used by the service provider as feedback information for billing purposes.

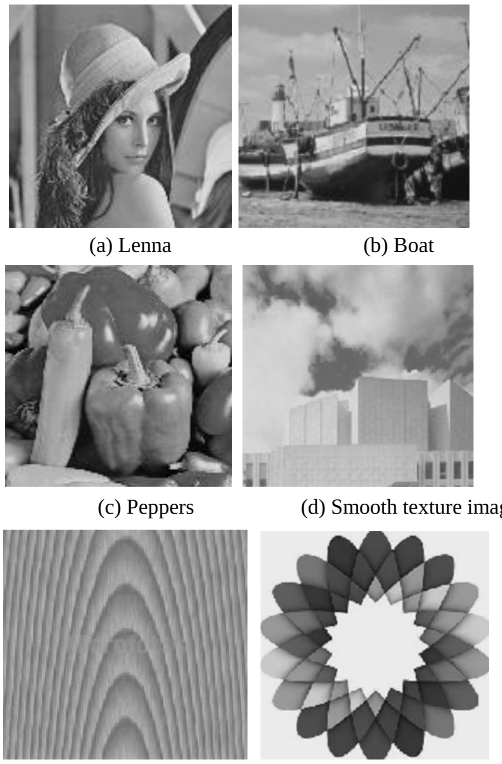

(a) Lenna (b) Boat

(c) Peppers (d) Smooth texture image

(e) Rough texture image (f) Regular image

Figure 5. Original images.

IV. Simulation Results

In this section, some experimental results characterizing the effectiveness of the proposed scheme are presented. The JPEG standard images "Lenna", "Boat", "Peppers", smooth texture image, rough texture image and regular image employed in our experiments have been properly chosen in order to simulate a multimedia service. The original images are shown in Fig. 5. In general, the effect degree of changed watermark blocks is greater than that of wrong blocks, so β should be greater than α from the theoretical view. In our experiments, α =2, β =3. We embed the watermark into the quantized DCT coefficients, and then we perform JPEG coding. The obtained bitstream is transmitted over a noisy channel which is simulated by random transmission errors with range 10^{-5}~3×10^{-3}. Let the encoded bitstream transmits 20 times at a certain BER, and note down *AF* and PSNR values, and finally the average of 20 pairs of values are as this image's *AF* and PSNR at this BER.

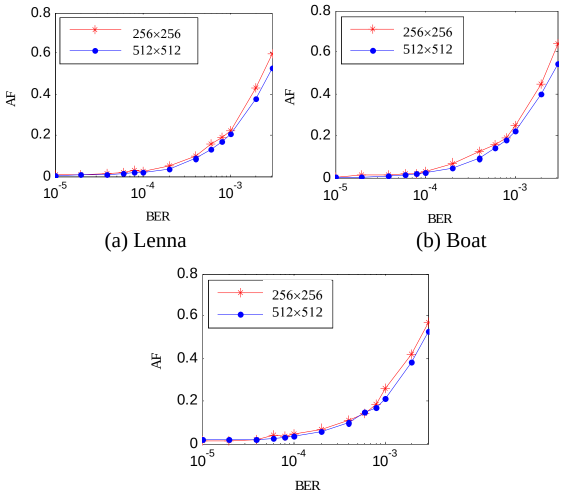

(a) Lenna (b) Boat

(c) Peppers

Figure 6. Assessment factors versus BER for a standard image with different size.

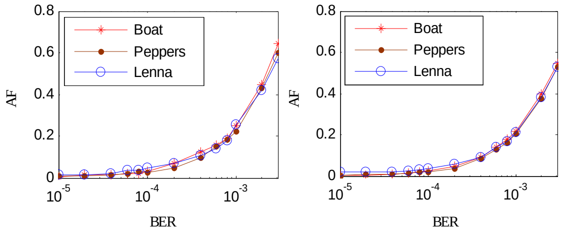

(a) 256×256 (b) 512×512

Figure 7. Assessment factors versus the BER for different standard images with same size.

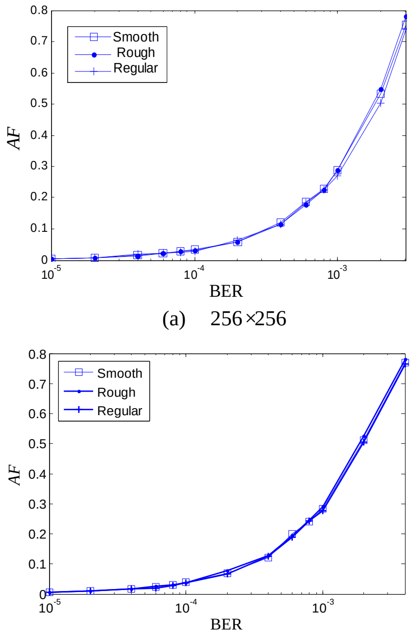

(a) 256×256

(b) 512×512

Figure 8. Assessment factors versus the BER for different texture images with same size.

Fig. 6 and Fig. 7 show the relation of BER and assessment factor *AF* for "Lenna", "Boat" and "Peppers" images with different size and image content. It can be seen that the assessment factor for each image increases when the BER increases. Besides, the image size and content don't affect this kind of relation. In order to further characterize the performances of the proposed scheme to provide a quality measure of the received image after the coding/transmission process, the relation of *AF* and BER for different texture images has been considered. Fig. 8 shows the assessment factors *AF* versus the BER for different texture images sized 256×256 and 512×512, respectively. The results are similar to the relations presented in Fig. 6 and Fig. 7. Besides, the image size and texture of images don't affect the relation of *AF* and BER. In order to further validate the rationality of resulting relations, we provide the received watermarked image against the different BER of the transmission channel in Fig. 9. It can be easily seen from these figures, the quality of received images is degraded when the BER increases. This is in accordance with the perceptual degradation that the image suffers at increasing BER. Besides, we test the PSNR which provides the qualitative assessments for the quality of images versus the BER. Fig. 10 shows the PSNRs for different images. It can be seen that the PSNR values decrease when the BER increases. This is in accordance with the results of assessment factors *AF* versus the BER.

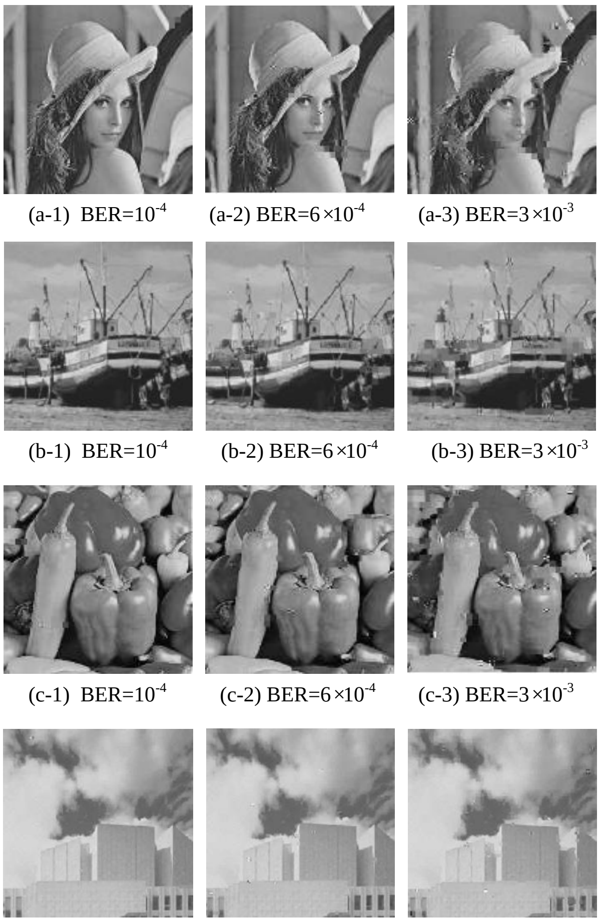

(a-1) BER=10^{-4} (a-2) BER=6×10^{-4} (a-3) BER=3×10^{-3}

(b-1) BER=10^{-4} (b-2) BER=6×10^{-4} (b-3) BER=3×10^{-3}

(c-1) BER=10^{-4} (c-2) BER=6×10^{-4} (c-3) BER=3×10^{-3}

(d-1) BER=10^{-4} (d-2) BER=6×10^{-4} (d-3) BER=3×10^{-3}

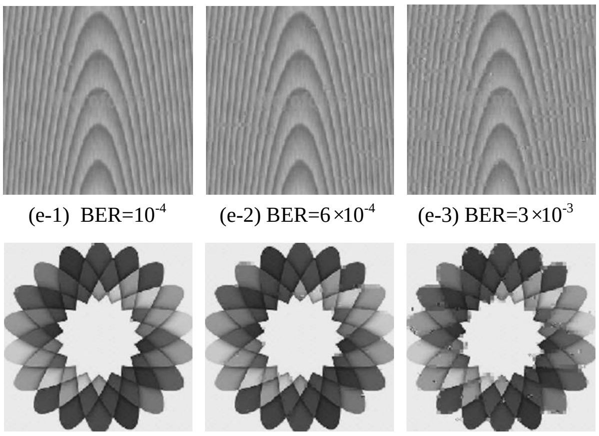

(e-1) BER=10^{-4} (e-2) BER=6×10^{-4} (e-3) BER=3×10^{-3}

(f-1) BER=10^{-4} (f-2) BER=6×10^{-4} (f-3) BER=3×10^{-3}

Figure 9. Received watermarked images against the different BER of the transmission channel.

The experimental results that have been presented validate the initial hypothesis that *AF* can be used to evaluate the image degradation extent and the transfer quality. Fig. 11 shows the average assessment factors *AF* of six images with different BERs. In [10], the authors partitioned the quality of channel transmission into three degrees by tracing watermark's alterations suffered by the data through the communication channel. In this paper, we classify the quality of channel transmission according to the resulting *AF* value. Namely, $AF \le 0.05$ is corresponding to the first-degree quality, $0.05 < AF \le 0.15$ is corresponding to the second-degree quality, and $AF > 0.15$ is corresponding to the third-degree quality. Specially, when $AF > 3$, the restored image is not ideal very much by a large number of experiments. Therefore, *AF* value can be as a reference of billing systems related to the quality of the services supplied.

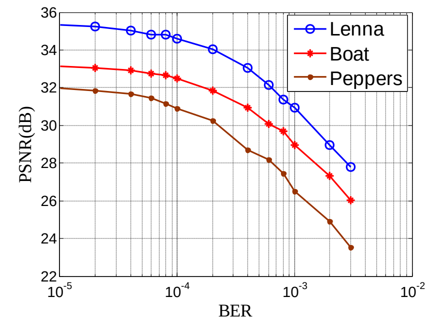

(a) Different standard images

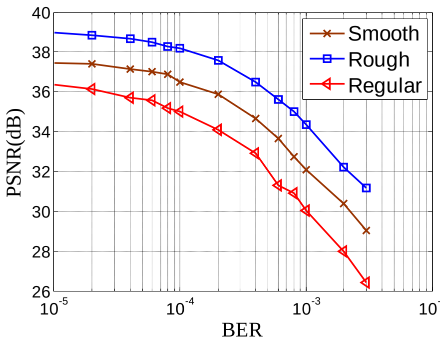

(b) Different texture images

Figure 10. The PSNRs versus the BER for different images.

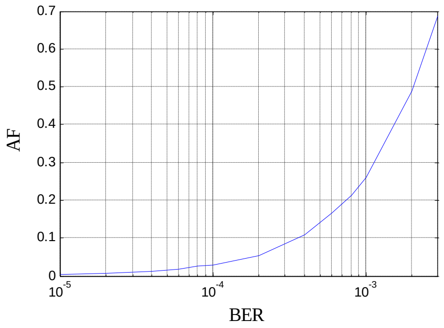

Figure 11. Average assessment factors versus the BER for six images.

V. CONCLUSIONS

In this paper, an unconventional use of digital watermarking has been proposed to blindly estimate the QoS of wireless image communications. In our method, a compressed-domain watermarking scheme is firstly designed, and the watermark is hidden into host image transfer stream. Tracing watermarking has been adopted as a technique to provide a blind measure of the QoS of the image communication link. The performance of the proposed method has been analyzed by the simulation trials. Experimental results show that the resulting assessment factor is very sensitive to the BER of channels, and the bit rate cannot be increased for data transmission. So the proposed scheme can be exploited for the application of QoS assessment in wireless image communications. In addition, it can be usefully employed for a number of different purposes in wireless image communication networks such as control feedback to the sending user on the effective quality of the link, detailed information to the operator for billing purposes and diagnostic information to the operator about the communication link status.

REFERENCES

[1] H. G. Wang, M. Hempel, D. M. Peng, W. Wang, H. Sharif, and H. H. Chen, "Index-based selective audio encryption for wireless multimedia sensor networks," *IEEE Transactions on Multimedia*, vol. 12, no. 3, pp. 215-223, April 2010.

[2] W. Wang, D. M. Peng, H. G. Wang, H. Sharif, and H. H. Chen, "A Multimedia quality-driven network resource management architecture for wireless sensor networks with stream authentication," *IEEE Transactions on Multimedia*, vol. 12, no. 5, pp. 439-447, August 2010.

[3] L. H. Tian, N. N. Zheng, J. R. Xue, and X. F. Wang, "An integrated visual saliency-based watermarking approach for synchronous image authentication and copyright protection," *Signal Processing: Image Communication*, vol. 26, no. 8-9, pp. 427-437, Oct 2011.

[4] H. X. Wang and M. Q. Fan, "NDFT-based image steganographic scheme with discrimination of tampers," *KSII Trans. on Internet and Information Systems*, vol. 5, no. 12, pp. 2340-2354, Dec. 2011.

[5] H. X. Wang and C. X. Liao, "JPEG images authentication with discrimination of tampers on the image content or watermark," *IETE Technical Review*, vol. 27, no. 3, pp. 244-251, May 2010.

[6] P. Campisi, M. Carli, G. Giunta, and A. Neri, "Blind quality assessment system for multimedia communication using tracing watermarking," *IEEE Trans. on Signal Processing*, vol. 51, no. 4, pp. 996-1002, Apr. 2003.

[7] F. Benedetto, G. Giunta, and A. Neri, "QoS assessment of 3G video-phone calls by tracing watermarking exploiting the new color space 'YST'," *IET Communications*, vol. 1, no. 4, pp. 696-704, Apr. 2007.

[8] F. Benedetto, G. Giunta, and A. Neri, "A business model founded on bayes' decision procedure for video-call billing from the estimated end-to-end QoS," in *Proc. IEEE 18th International Symposium on Personal, Indoor and Mobile Radio Communications*, pp. 1-5, Sept. 2007.

[9] F. Benedetto, A. Curcio, G. Giunta, and A. Neri, "A Bayesian business model for video-call billing for end-to-end QoS provision," *IEEE Trans. on Vehicular Technology*, vol. 58, no. 2, pp. 836-842, Feb 2009.

[10] D. Zheng, J. Y. Zhao, W. J. Tam, and F. Speranza, "Image quality measurement by using digital watermarking," in *Proc. 2nd IEEE International Workshop on Haptic, Audio and Visual Environments and Their Applications Digital Object*, pp. 65-70, Sept 2003.

[11] X. P. Zhang, S. Z. Wang, Z. X. Qian, and G. R. Feng, "Reversible fragile watermarking for locating tampered blocks in JPEG images," *Signal Processing*, vol. 90, no. 12, pp. 3026-3036, Dec. 2010.

[12] D. Caragata, A. L. Radu, S .El Assad, and C. Apostol, "Chaos based fragile watermarking algorithm for JPEG images," in *Proc. International Conference on Internet Technology and Secured Transactions*, pp. 1-7, Nov. 2010.

[13] M. Iwata, K. Miyake, and A. Shiozaki, "Digital watermarking method to embed index data in JPEG images," *IEICE Trans. on Fundamentals*, vol. E85-A, no. 10, pp. 2267-2271, Oct 2002.

[14] JPEG. [Online]. Available: http://en.wikipedia.org/wiki/JPEG

[15] O. Kahn, S. Division, and M. Ye, *JPEG/MPEG 2 Technology*, Beijing: Science Press, 2004, pp. 187-195.

Hongxia Wang received the B.S. degree from Hebei Normal University, Shijiazhuang, in 1996, and the M.S. and Ph.D. degrees from University of Electronic Science and Technology of China, Chengdu, in 1999 and 2002, respectively. She engaged in postdoctoral research work in Shanghai Jiaotong University from 2002 to 2004. Currently she is a professor with School of Information Science and Technology, Southwest Jiaotong University, Chengdu. Her research interests include multimedia information security, digital forensics, information hiding and digital watermarking. She has published 60 peer research papers and wined 8 authorized patents.

Bangxu Yin received the B.S. and M.S. degrees from Southwest Jiaotong University, Chengdu, in 2006 and 2011, respectively. He is currently pursuing the Ph.D. degree with Southwest Jiaotong University. His research interests include multimedia information security and network security.